Available online at www.sciencedirect.com
SCIENCE DIRECT
Plant Physiology and Biochemistry 44 (2006) 171–180
Plant Physiology and Biochemistry
www.elsevier.com/locate/plaphy

Research article

# Characterization and expression of Arabidopsis UDP-sugar pyrophosphorylase

L.A. Litterer [a], J.A. Schnurr [b], K.L. Plaisance [a], K.K. Storey [a], J.W. Gronwald [b,*], D.A. Somers [a,c]

[a] *Department of Agronomy and Plant Genetics, University of Minnesota, 411 Borlaug Hall, 1991 Upper Buford Circle, St. Paul, Minnesota 55108, United States*
[b] *USDA-ARS, Plant Science Research, St. Paul, Minnesota 55108, United States*
[c] *Current address: Monsanto Company, Agracetus Campus, Middleton, WI 53562, United States*

Received 28 November 2005
Available online 17 May 2006

**Abstract**

At5g52560, a homolog of pea (*Pisum sativum*) UDP-sugar pyrophosphorylase (*PsUSP*) was functionally annotated by expression in *Escherichia coli* and subsequent characterization of substrate specificity and kinetic properties. Arabidopsis contains a single *USP* gene (*AtUSP*) and evaluation of gene databases suggests that *USP* is unique to plants. The 69 kDa *AtUSP* gene product exhibited high activity with Glc-1-P, GlcA-1-P and Gal-1-P, but low activity with GlcNAc-1-P, Fuc-1-P, Man-1-P, inositol-1-P or Glc-6-P. AtUSP was activated by magnesium and preferred UTP as co-substrate. Apparent $K_m$ values for GlcA-1-P, Glc-1-P and UTP were 0.13 mM, 0.42 mM and 0.14 mM, respectively. In the reverse direction (pyrophosphorolysis), the apparent $K_m$ values for UDP-GlcA, UDP-Glc and pyrophosphate were 0.56 mM, 0.72 mM and 0.15 mM, respectively. USP enzyme activity (UDP-GlcA → GlcA-1-P) was detected in Arabidopsis tissues with highest activity found in the inflorescence. As determined by semi-quantitative RT-PCR, *AtUSP* transcript is widely expressed with high levels detected in the inflorescence. To evaluate tissue-specific expression of *AtUSP*, histochemical GUS staining of plants transformed with *AtUSPprom:GUS* constructs was performed. In 7-day-old seedlings, GUS staining was detected in cotyledons, trichomes and vascular tissues of the primary root. In the inflorescence of older plants, high levels of GUS staining were detected in cauline leaves, the epidermis of the stem and in pollen. *In silico* analysis of *AtUSP* expression in developing pollen indicates that transcript levels increase as development proceeds from the uninucleate to the tricellular stage. The results suggest that *AtUSP* plays an important role in pollen development in Arabidopsis.
© 2006 Elsevier SAS. All rights reserved.

*Keywords:* Arabidopsis thaliana; Cell wall; Pyrophosphorylase; UDP-glucuronic acid; UDP-glucose; UDP-sugar pyrophosphorylase

## 1. Introduction

Plant cell walls consist of cellulose, matrix polysaccharides (pectin and hemicellulose), phenolics and glycoproteins [3,8]. Matrix polysaccharides make up more than 60% of the primary cell wall of Arabidopsis leaves [36]. The amount and composition of cell wall matrix polysaccharides influence the quality of food and fiber produced by crop plants. For example, the pectin content of forage cell walls is important in determining nutritional value for ruminants [29]. The tools of molecular biology can be used to develop transgenic plants that exhibit desirable modifications in the amount and composition of cell wall matrix polysaccharides. However, progress in this area is limited by lack of understanding of key enzymes regulating pectin and hemicellulose biosynthesis.

UDP-GlcA is a major precursor for nucleotide sugars (UDP-GalA, UDP-Xyl, UDP-Ara) that are incorporated into pectin and hemicellulose [12]. Despite its importance in matrix polysaccharide biosynthesis, the regulation of UDP-GlcA synthesis is poorly understood. As seen in Fig. 1, UDP-GlcA can be synthesized by two distinct pathways in plants: (1) the nucleotide sugar oxidation (NSO) pathway where UDP-Glc dehydrogenase catalyzes the oxidation of UDP-Glc, or (2) the *myo*-inositol oxidation (MIO) pathway which involves reactions cat-

*Abbreviations:* Ara, arabinose; Fuc, fucose; Gal, galactose; Glc, glucose; GlcA, glucuronic acid; GlcNAc, N-acetylglucosamine; GUS, β-glucuronidase; Man, mannose; PPi, pyrophosphate; UDP, uridine diphosphate; USP, UDP-sugar pyrophosphorylase; Xyl, xylose.

* Corresponding author. Tel.: +1 612 625 8186; fax: +1 651 649 5058.
*E-mail address:* gronw001@umn.edu (J.W. Gronwald).

0981-9428/$ - see front matter © 2006 Elsevier SAS. All rights reserved.
doi:10.1016/j.plaphy.2006.04.004

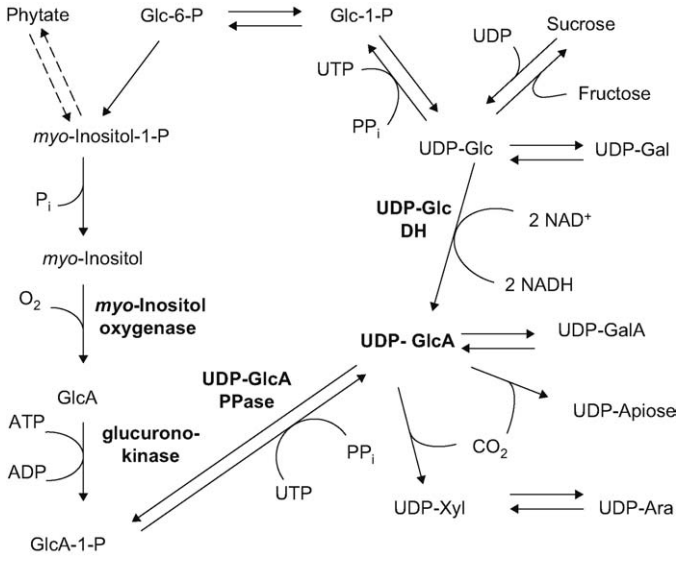


Fig. 1. Nucleotide sugar biosynthesis pathways in plants adapted from Feingold and Avigad [12] showing the *myo*-inositol oxidation and UDP-Glc dehydrogenase pathways for UDP-GlcA synthesis. Abbreviations: Glc, glucose; Gal, galactose; GlcA, glucuronic acid; GalA, galacturonic acid; Xyl, xylose; Ara, arabinose; UDP-Glc DH, UDP-glucose dehydrogenase; UDP-GlcA PPase, UDP-GlcA pyrophosphorylase.

alyzed by *myo*-inositol oxygenase, glucuronokinase and UDP-GlcA pyrophosphorylase (EC 2.7.7.44) [12,23]. UDP-Glc dehydrogenase is present in plants [17,21,33], mammals [32] and prokaryotes [25], and its properties have been well characterized. In contrast, the terminal enzyme of the *myo*-inositol oxidation pathway, UDP-GlcA pyrophosphorylase, is unique to plants and its regulation is poorly understood [23].

Our current knowledge of UDP-GlcA pyrophosphorylase is based on activity measured in partially purified fractions from seedlings of mung bean (*Phaseolus aureus* L.) [13], barley (*Hordeum vulgare* L.), broad bean (*Vicia faba* L.) and pea (*Pisum sativum* L.) [27,28]; maize (*Zea mays* L.) seedlings and endosperm [10]; pollen of lily (*Lilium longiflorum* L.) [10] and common cattail (*Typha latifolia* L.) [18]; and liverwort (*Riella helicophylla* L.) [35]. Because these studies were conducted with semi-purified enzyme fractions, our understanding of the properties of UDP-GlcA pyrophosphorylase is incomplete. Earlier studies indicated that the enzyme has a pH optimum in the range of 8.0 to 9.0, is specific for UTP as co-substrate and requires divalent cations for activity [18,27]. However, in only two reports was cross-reactivity with other monosaccharide-1-P sugars examined. The ammonium sulfate fraction characterized from mung bean exhibited activity with both GlcA-1-P and GalA-1-P [13]. The semi-purified UDP-GlcA pyrophosphorylase from barley seedlings did not exhibit cross-reactivity with Glc-1-P [27]. In addition, there is uncertainty about the molecular wt of UDP-GlcA pyrophosporylase. UDP-GlcA pyrophosphorylase from common cattail pollen has a molecular wt of approximately 71 kDa [18]. In contrast, the enzyme from barley seedlings [27] has a molecular wt of approximately 35 kDa. Thus, both molecular wt and substrate range of UDP-GlcA pyrophosphorylase are uncertain.

Recently, Kotake et al. [22] purified and characterized a broad substrate UDP-sugar pyrophosphorylase (USP) from pea. A comparison of various monosaccharide-1-P substrates indicated that the highest activity occurred with Glc-1-P, GlcA-1-P, Gal-1-P and Ara-1-P. The recombinant PsUSP was also characterized and found to have the same properties as the purified enzyme. Kotake et al. [22] proposed that PsUSP plays an important role in the salvage pathway for the synthesis of nucleotide sugars. In this pathway, monosaccharides released during degradation of glycoconjugates and polysaccharides are recycled back into the UDP-sugar pool. Homologs of Ps*USP* were identified in rice (*Oryza sativa* L.) (AK064009) and Arabidopsis (At5g52560) [22].

The objectives of this study were to: (1) functionally annotate the putative *USP* from Arabidopsis (*AtUSP*), including characterization of kinetic parameters with substrates, and (2) investigate its expression in various tissues of Arabidopsis. Recombinant AtUSP exhibits similarities, but also significant differences compared to recombinant PsUSP [22]. Both transcripts and enzyme activity of *AtUSP* are widely expressed in Arabidopsis. Histochemical GUS staining of inflorescences of plants transformed with a *AtUSPprom:GUS* construct indicated high expression of *AtUSP* in pollen. The possibility that AtUSP serves as UDP-GlcA pyrophosphorylase, the terminal enzyme in the MIO pathway, is discussed.

## 2. Results

### 2.1. Functional annotation of AtUSP

Kotake et al. [22] identified At5g52560 as a homolog of the broad substrate UDP-sugar pyrophosphorylase (PsUSP) characterized in pea. PsUSP and the putative Arabidopsis UDP-sugar pyrophosphorylase, AtUSP (At5g52560), share 80% identity (nucleotide) and the predicted proteins share 77% identity and 88% similarity [22]. *AtUSP* has an open reading frame of 1842 bp that encodes a predicted protein of 614 amino acids. Sequence analysis using TargetP [11] predicted that AtUSP is a cytosolic protein because an identifiable target sequence was not found.

To functionally annotate At5g52560, the coding region was cloned by RT-PCR, inserted into pET28, expressed in *Escherichia coli* and purified. His-tag affinity purification of putative AtUSP yielded a single peptide that migrated at approximately 70 kDa on SDS-PAGE (Fig. 2, lane 1). The N-terminal 17 amino acids which included the poly-His motif were cleaved from the fusion peptide using thrombin. The size of the thrombin-cleaved, purified putative AtUSP was 69 kDa, consistent with removal of the His-tag (Fig. 2, lane 2). All enzyme characterization was done with thrombin-treated putative AtUSP to more accurately assess enzyme characteristics *in planta*. The purified enzyme was labile in elution buffer containing 0.5 M imidazole. Most enzyme activity (90%) was lost within 16 h of storage in elution buffer (4 °C). However, desalting into a buffer containing 20% (w/v) sucrose, 50 mM

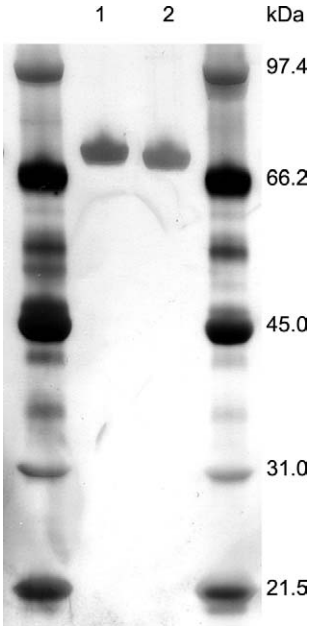


Fig. 2. Silver-stained SDS-PAGE gel of purified AtUSP fusion protein. Numbers indicate the positions of molecular weight markers on 4–12% acrylamide gel. Lane 1: 100 ng fusion protein eluted from His-Tag affinity column; lane 2: 100 ng protein after thrombin cleavage and purification.

TAPS (pH 8.0), 1 mM $MgCl_2$ and 1 mM DTT stabilized the enzyme for several days at 4 °C.

Putative AtUSP was assayed in the forward direction with various sugar phosphates (Table 1). High levels of activity were measured with Glc-1-P, GlcA-1-P or Gal-1-P as substrates. In contrast, GlcNAc-1-P, Fuc-1-P, Man-1-P, inositol-1-P and Glc-6-P exhibited very low activity. Currently, the *AtUSP* mRNA sequences available through GenBank are annotated as an unknown protein (AF360236, AY040035) or as a gene with sequence similarities with the pea *PsUSP* (NM124635). The results presented here functionally annotate AtUSP as a broad substrate UDP-sugar pyrophosphorylase and confirm that *AtUSP* is a homolog of *PsUSP*.

Table 1
Relative activity of AtUSP with various sugar phosphate substrates

| Substrate | Relative Activity |
|---|---|
| GlcA-1-P | 100 |
| Glc-1-P | 130.0 ± 5.4 |
| Gal-1-P | 76.8 ± 2.4 |
| GlcNAc-1-P | 6.3 ± 1.5 |
| Fuc-1-P | 3.4 ± 1.7 |
| Man-1-P | 2.0 ± 0.6 |
| Inositol-1-P | 7.0 ± 0.6 |
| Glc-6-P | 3.6 ± 1.2 |

Specific activity was determined in the forward direction by detection of PPi produced in the presence of 1 mM UTP, 2 mM $MgCl_2$, 1 mM of the indicated sugar phosphate and inorganic pyrophosphorylase, relative to specific activity with GlcA-1-P (32.1 ± 3.0 μmol $min^{-1}$ $mg^{-1}$) set at 100%. Values are means ± SE ($N = 3$).

Activity with the pentose sugars Xyl-1-P and Ara-1-P was not examined because they are not commercially available. Instead, we examined the ability of UDP-Xyl, UDP-Ara and UDP-Glc to serve as competitive inhibitors of the pyrophosphorolysis of UDP-GlcA (Table 2). Addition of 1 mM UDP-Xyl to a standard reaction mixture containing 1 mM UDP-GlcA reduced UDP-GlcA pyrophosphorylase activity by 5%, addition of 1 mM UDP-Ara reduced activity by 13%, and addition of 1 mM UDP-Glc reduced activity by 23%. If two sugars are equally effective as substrates, each would potentially reduce activity for the other by 50% in this assay. We also examined whether 1 mM UDP-Xyl, UDP-Ara or UDP-GlcA were competive inhibitors of the pyrophosphorolysis of UDP-Glc. Addition of 1 mM UDP-Xyl to a standard reaction mixture containing 1 mM UDP-Glc reduced UDP-Glc pyrophosphorylase activity by 17%, addition of UDP-Ara reduced activity by 22%, and addition of UDP-GlcA reduced activity by 75%. From this data, we can conclude that UDP-GlcA is a more competitive inhibitor of UDP-Glc pyrophosphorylase activity than UDP-Glc is of UDP-GlcA pyrophosphorylase activity. Our results also show that AtUSP exhibits lower affinity for UDP-Ara and UDP-Xyl compared with UDP-GlcA or UDP-Glc, and that affinity is higher for UDP-Ara than for UDP-Xyl. Based on the substrates examined, our results indicate that the preferred substrates of AtUSP are GlcA-1-P (forward reaction) and UDP-GlcA (reverse reaction).

A comparison of nucleotide triphosphate preference indicated that UDP-GlcA pyrophosphorylase activity was specific for UTP (Table 3). Activity in the presence of other nucleotide triphosphates (ATP, CTP or GTP) was less than 10% of that measured in the presence of UTP. Similar to other pyrophosphorylases, AtUSP activity required divalent cations. No activity was detected when 20 mM EDTA was added to the assay. When assayed at 2 mM, magnesium and manganese resulted in equivalent activation; no activity was detected in the presence of calcium (2 mM) (data not shown). Effects of temperature on enzyme activity were evaluated over the range of 15-55 °C. Maximum activity was obtained at 45 °C, with a rapid drop in activity at higher temperatures (data not shown). Enzymatic activity for the forward reaction (UDP-GlcA forma-

Table 2
Comparison of the effect of various UDP-sugars on UDP-GlcA and UDP-Glc pyrophosphorylase activity of AtUSP[a]

| Added competing substrate | UDP-GlcA pyrophosphorylase activity | | UDP-Glc pyrophosphorylase activity | |
|---|---|---|---|---|
| | *μmol $min^{-1}$ $mg^{-1}$* | *%* | *μmol $min^{-1}$ $mg^{-1}$* | *%* |
| None | 52.4 ± 2.5 | 100 | 57.8 ± 1.9 | 100 |
| UDP-Glc | 40.4 ± 2.0 | 77 | – | – |
| UDP-GlcA | – | – | 14.6 ± 3.5 | 25 |
| UDP-Xyl | 49.6 ± 0.8 | 95 | 47.8 ± 3.4 | 83 |
| UDP-Ara | 45.6 ± 4.2 | 87 | 45.2 ± 0.7 | 78 |

[a] Activity was determined in the reverse direction by measuring [$^{14}$C]Glc-1-P or [$^{14}$C]GlcA-1-P production in a reaction containing 5 mM NaPPi, 2 mM $MgCl_2$, 1 mM UDP-[$^{14}$C]Glc or UDP-[$^{14}$C]GlcA plus 1 mM UDP-sugar (when added). Values are means ± SE ($N = 3$).

Table 3
Relative activity of AtUSP with various nucleotide triphosphates

| Substrate | Relative activity |
|---|---|
| UTP | 100 |
| ATP | 5.3 ± 2.1 |
| CTP | 5.1 ± 2.0 |
| GTP | 8.8 ± 2.6 |

Specific activity was determined in the forward direction by detection of PPi produced in the presence of 1 mM GlcA-1-P, 2 mM $MgCl_2$ and 1 mM of the indicated nucleotide. Values are means ± SE ($N = 3$).

tion) was tested over a wide range of pH values. The pH curve showed a broad optima between 7.5 and 8.5 with no activity at or below pH 5.0 (data not shown).

Kinetic parameters of AtUSP were determined in both the forward and reverse directions for GlcA-1-P and Glc-1-P (Table 4). Although $V_{max}$ for the forward reaction was greater with Glc-1-P compared to GlcA-1-P, the $K_m$ for GlcA-1-P was three-fold lower than for Glc-1-P. In contrast, the affinity for UTP was only slightly greater with GlcA-1-P as substrate compared to Glc-1-P. The $k_{cat}/K_m$ values for GlcA-1-P and Glc-1-P were 3. $1 \times 10^5$ $s^{-1}$ $M^{-1}$ and 1. $6 \times 10^5$ $s^{-1}$ $M^{-1}$, respectively, indicating that the catalytic efficiency of USP was greater with GlcA-1-P as substrate compared to Glc-1-P. In the reverse direction, the $K_m$ for UDP-GlcA was 0.56 mM while the $K_m$ for UDP-Glc was 0.72 mM. These results are in agreement with the substrate competition experiments (Table 2) that indicated higher affinity for UDP-GlcA compared to UDP-Glc.

### 2.2. USP Homologs

*AtUSP* appears to be a single gene in Arabidopsis as no obvious homologs are present in the genome. A search of both genomic and expressed sequences indicated that more than 20 plant species have putative *AtUSP* homologs that are 70 to 80% identical and 80 to 95% similar. Although USP has been identified in both dicots and monocots, we found no obvious *AtUSP* homologs in fungi, bacteria, archaea or metazoa.

*AtUSP* is only moderately similar to other members of the Arabidopsis pyrophosphorylase family. The most closely related Arabidopsis genes are the two putative UDP-GlcNAc pyrophosphorylases (At1g31070, At2g35020) with 42% similar and 26% identical amino acids. The region of homology with UDP-GlcNAc pyrophosphorylases covers the N-terminal 355 residues of both peptides. *AtUSP* is less closely related to the two putative UDP-Glc pyrophosphorylases (At3g03250, At5g17310) with 35% similar and 23% identical amino acids, respectively. Homology with the Arabidopsis UDP-Glc pyrophosphorylases begins approximately 50 residues downstream of the N-terminus of At5g52560 and extends to aa 403. The C-terminal third of AtUSP has no similarity to any annotated pyrophosphorylase in GenBank but contains a 64 aa motif shared with microtubule-associated protein MAP65-1a (GenBank NP_567756).

### 2.3. USP enzyme activity and transcript levels

USP enzyme activity was measured in the reverse direction (UDP-GlcA → GlcA-1-P) in crude extracts of Arabidopsis seedlings, the rosettes of 2 to 5-wk-old plants and the inflorescences of 35-day-old plants (Table 5). USP activity was present in extracts of all tissues tested, but highest activity was detected in the inflorescence. In these same tissues, *AtUSP* transcript levels were quantified by semi-quantitative RT-PCR. *AtUSP* transcripts were present in all tissues tested and were most abundant in rosettes of 21-day-old plants and the inflorescences of 35-day-old plants (Table 5).

### 2.4. AtUSP promoter activity and in silico analysis

To determine tissue-specific activity of the USP promoter, we amplified 2 kb of sequence upstream of the start codon in *AtUSP* and cloned it into pBI101.1, a promoterless-GUS construct. Two independent transformants were used for the ana-

Table 5
*AtUSP* transcript level and enzyme activity in Arabidopsis tissue extracts

| Tissue | Age (days) | Transcript[a] | Activity[b] |
|---|---|---|---|
| Seedling | 7 | 0.65 ± 0.03 | 141.2 ± 4.1 |
| Rosette | 14 | 0.64 ± 0.02 | 173.8 ± 13.9 |
| Rosette | 21 | 0.83 ± 0.11 | 184.5 ± 3.3 |
| Rosette | 28 | 0.63 ± 0.03 | 190.9 ± 5.5 |
| Rosette | 35 | 0.62 ± 0.01 | 168.0 ± 6.7 |
| Inflorescence | 35 | 0.76 ± 0.09 | 341.4 ± 6.0 |

[a] Relative transcript abundance was determined by semi-quantitative, multiplexed RT-PCR. Values represent the mean ± SE of band intensities of USP compared to 18S RNA transcript levels for three separate RNA extractions.

[b] AtUSP activity from desalted crude extracts of various tissues. Activity was measured in the reverse direction (PPi + [$^{14}$C]UDP-GlcA → [$^{14}$C]GlcA-1-P + UTP) and reported as nmol $min^{-1}$ g fresh $weight^{-1}$. Values represent mean ± SE of triplicate extractions assayed in duplicate.

Table 4
Kinetic parameters for forward and reverse reactions of AtUSP for UDP-GlcA and UDP-Glc pyrophoshorylase activity[a]

| Reaction | Substrate A | Substrate B | $V_{max}$ | $K_A$[b] | $K_B$[c] |
|---|---|---|---|---|---|
| | | | *nmol min$^{-1}$* | *mM* | *mM* |
| Forward | GlcA-1-P | UTP | 3.47 ± 0.18 | 0.13 ± 0.02 | 0.14 ± 0.02 |
| | Glc-1-P | UTP | 5.76 ± 0.38 | 0.42 ± 0.05 | 0.19 ± 0.02 |
| Reverse | UDP-GlcA | PPi | 4.25 ± 0.17 | 0.56 ± 0.12 | 0.15 ± 0.02 |
| | UDP-Glc | PPi | 4.95 ± 0.53 | 0.72 ± 0.17 | 0.16 ± 0.07 |

[a] Kinetic parameters for AtUSP in the forward direction (formation of UDP-sugars) were measured at five concentrations of each substrate and the Michaelis constants were calculated by non-linear regression. Rates in the reverse direction were determined with saturating conditions for one substrate (1 mM PPi, 2 mM UDP-GlcA, or 2 mM UDP-Glc). The data was fitted to the Michaelis-Menten equation using non-linear regression. Values for both the forward and reverse reactions are means ± SE ($N = 3$).

[b] $K_A = K_m$ value for substrate A.

[c] $K_B = K_m$ value for substrate B.

lysis of promoter activity. Histochemical GUS staining of segregating progeny from the two individuals revealed that in 7-day-old seedlings, GUS activity was present in cotyledons, trichomes of primary leaves and the vascular tissues within the basal portion of the root (Fig. 3A–D). Rosettes at 14 days exhibited GUS activity primarily in the trichomes of leaves and the vascular system of the petiole (Fig. 3E). Staining in rosettes of flowering plants was similar to that observed in 14-day-old plants (data not shown).

GUS expression was also observed in young stems of the inflorescence (Fig. 4A). As revealed in cross-section, GUS activity in stems was most intense in the epidermis with fainter staining also observed in xylem and phloem (Fig. 4B). The most intense GUS staining of the inflorescence occurred in cauline leaves, sepals, and anthers (Fig. 4A, C). In stamens, staining was limited to individual pollen grains (Fig. 4C, inset). The staining pattern that was observed is consistent with *in silico* expression data obtained through Genevestigator [37]. Fig. 5 summarizes the pattern of *AtUSP* transcript levels found in various tissues. *AtUSP* transcript is present in every tissue tested, with the highest signal intensity observed in stem and stamen (Fig. 5). Because histochemical GUS staining showed intense staining of pollen within the anther (Fig. 4C, inset), we analyzed *in silico* transcript levels within developing pollen. *AtUSP* transcript levels increased during pollen development, peaking at the tricellular stage (Fig. 6).

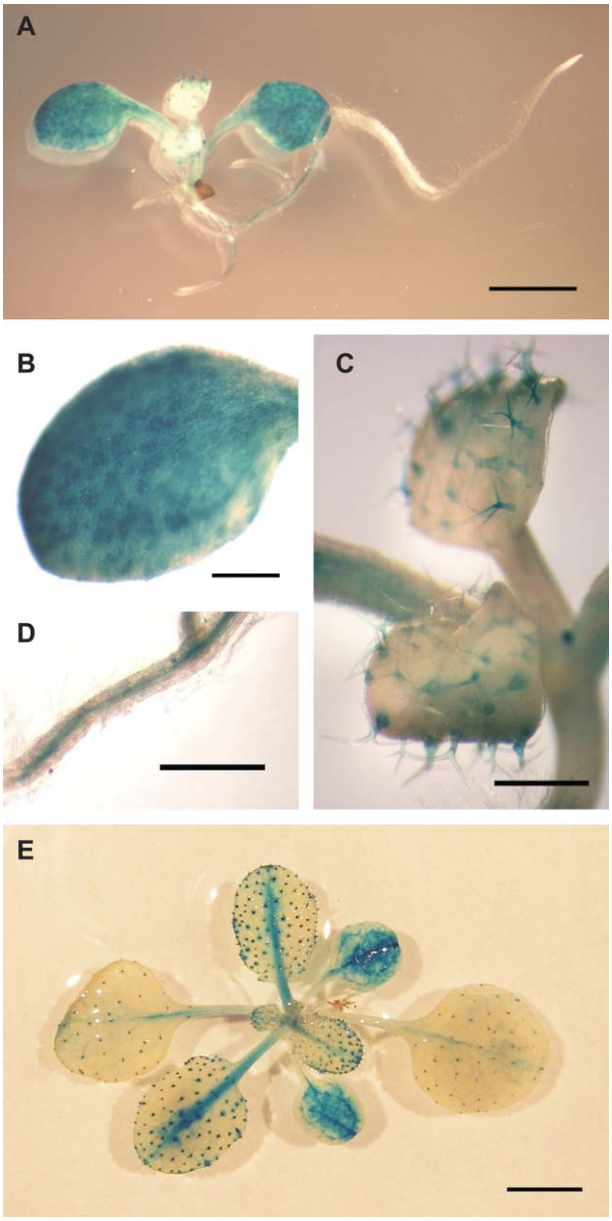


Fig. 3. Histochemical staining of young transgenic Arabidopsis containing a *AtUSPprom:GUS* construct. (A) 7-day-old-seedling, (B) close up of cotyledon in (A), (C) close up of developing first true leaves in (A) showing expression in trichomes, (D) close up of basal section of primary root shown in (A), (E) rosette of 14 day-old-seedling showing staining of trichomes and petioles. Scale for bars shown in Figures: 2 mm for (A) and (E), 0.5 mm for (B), (C) and (D).

## 3. Discussion

By functional annotation of *AtUSP* (At5g52560), we confirmed that the gene is a homolog of *PsUSP* [22]. Both genes encode broad substrate pyrophosphorylases that are similar in many respects. Both AtUSP and PsUSP exhibit: (1) high activity with GlcA-1-P, Glc-1-P and Gal-1-P, but little or no activity with GlcNAc-1-P, Man-1-P, Fuc-1-P, or Glc-6-P, (2) a temperature optimum of approximately 45 °C, and (3) similar $K_m$ values for Glc-1-P. However, there are significant differences between the two pyrophosphorylases. The relative in vitro activities of AtUSP are Glc-1-P > GlcA-1-P > Gal-1-P (Table 1). In contrast, the relative activities for PsUSP are Gal-1-P > Glc-1-P > GlcA-1-P [22]. Other differences between AtUSP and PsUSP are the $K_m$ values for GlcA-1P and UTP. The $K_m$ value for GlcA-1-P is significantly lower for AtUSP (0.13 mM) compared to PsUSP (0.48 mM). For UTP, the $K_m$ values are

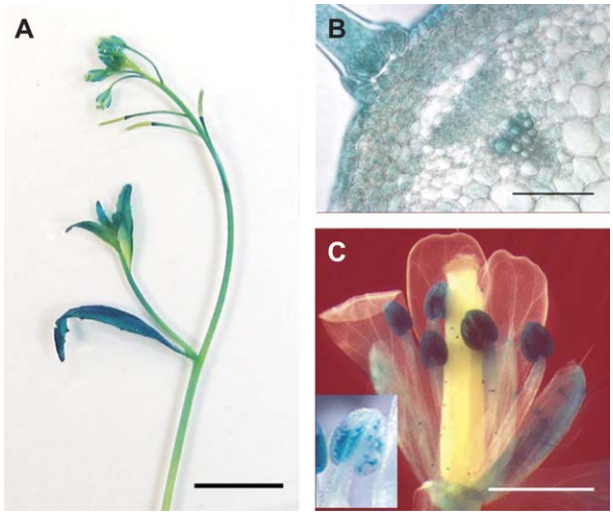


Fig. 4. Histochemical staining of older transgenic Arabidopsis containing a *AtUSPprom:GUS* construct. (A) inflorescence of 35 day-old-seedling showing GUS staining in cauline leaves, stem and flowers, (B) cross-section of stem showing staining of a trichome, the epidermis and vascular tissues, (C) close-up of flower showing staining of anthers, inset shows staining of pollen grains within anthers. Scale for bars shown in Figures: 1 cm for A, 0.1 mm for B, 1 mm for C.

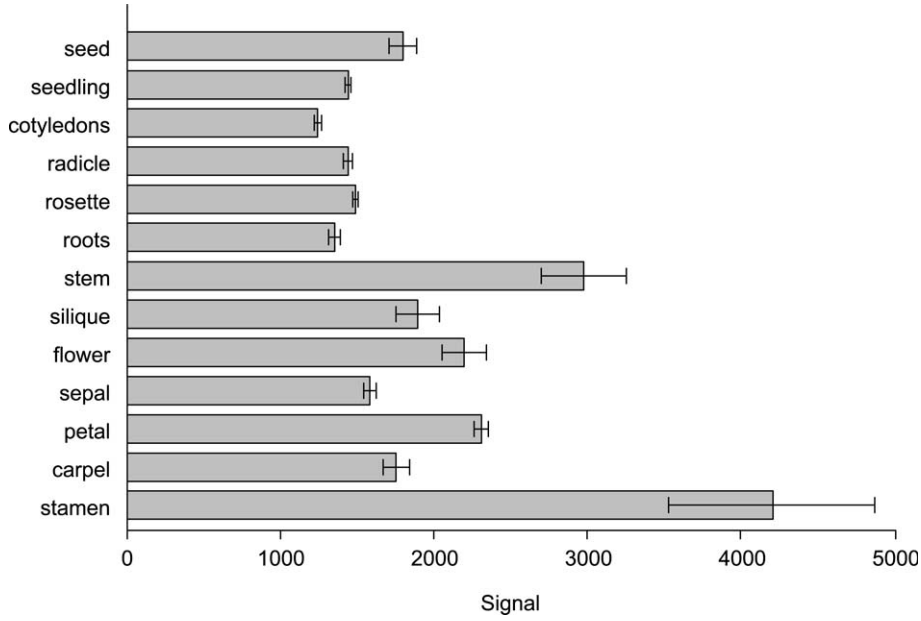


Fig. 5. *In silico* analysis of *AtUSP* transcript expression in various tissues. The data used to create the figure were obtained at https://www.genevestigator.ethz.ch/ [37].

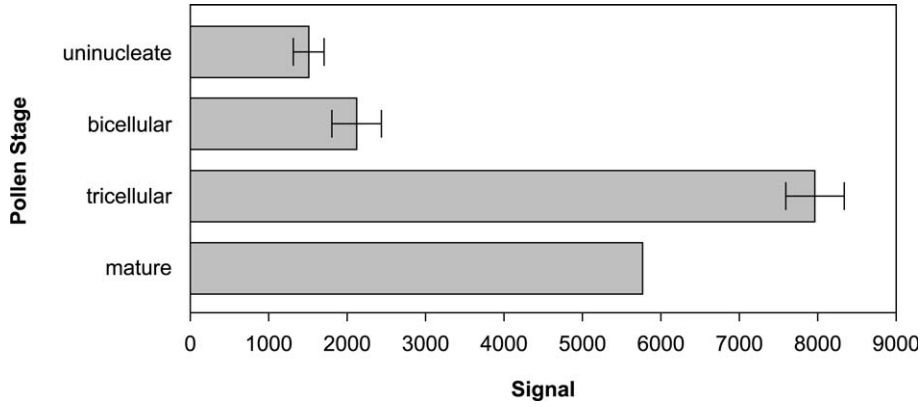


Fig. 6. *In silico* analysis of *AtUSP* transcript expression during pollen development from the uninucleate to the mature stage. The data used to create the figure were obtained at https://www.genevestigator.ethz.ch/ [37].

0.14 mM and 0.048 mM for AtUSP and PsUSP, respectively. The pH optimum for AtUSP and PsUSP also differ. PsUSP exhibits maximum activity between pH 6.5–7.5 while AtUSP exhibits maximum activity between pH 7.5–8.5 which is similar to plant UDP-Glc pyrophosphorylase [24,31].

The function of *USP* in plants is not clearly defined. On the basis of its broad substrate specificity, Kotake et al. [22] proposed that PsUSP plays a key role in the salvage pathway for synthesis of nucleotide sugars. The broad specificity of Arabidopsis USP for monosaccharide-1-P sugars (Table 1) and its wide expression in various tissues (Table 5, Figs. 3 and 4) are consistent with this role. In the salvage pathway, monosaccharides released during hydrolytic reactions involving polysaccharides and other glycoconjugates (glycoproteins, glycolipids) are converted to nucleotide sugars by a two-step process involving: (1) C-1 sugar kinase and (2) nucleotide diphosphate (NDP) sugar pyrophosphorylase [12]. Although the reaction catalyzed by NDP-pyrophosphorylase is reversible, it is believed to function in the forward direction (NDP-sugar formation) because of the high levels of pyrophosphatase found in plant cells [12]. There is evidence that the salvage pathway plays a role in recycling monosaccharides released from polysaccharides during cell wall synthesis and turnover [8,14,15]. Pulse-chase studies of cell wall polysaccharides indicate turnover of Ara and Gal [14–16].

Our results, based on UDP-sugar competition studies for the reverse reaction (pyrophosphorolysis) (Table 2), show that AtUSP exhibited lower affinity for UDP-Xyl compared to UDP-GlcA or UDP-Glc. For the forward reaction, PsUSP exhibited low activity and affinity for Xyl-1-P compared to GlcA-1-P or Glc-1-P [22]. Kotake et al. [22] proposed that USP may play a role in recycling Xyl via the salvage pathway. However, evidence in the literature suggests that this may not occur because xylose kinase is not found in plants [7,8,15]. Instead, Xyl is isomerized to xylulose and its carbons recycled via the pentose phosphate pathway [7,8,12].

In addition to its role in the salvage pathway for synthesis of nucleotide sugars, it is also possible that USP serves as UDP-GlcA pyrophosphorylase (EC 2.7.7.44), the terminal enzyme of the MIO pathway (Fig. 1). The gene for UDP-GlcA pyrophosphorylase has not been identified. The high activity and affinity of AtUSP for GlcA-1-P is consistent with this role. Based on determination of $K_m$ values for GlcA-1-P and Glc-1-P, and competition studies comparing the effects of UDP-sugars on the reverse reaction (pyrophosphorolysis), it appears that GlcA-1-P/UDP-GlcA are the preferred substrates for the forward and reverse reactions of AtUSP, respectively.

It is not clear whether UDP-GlcA pyrophosphorylase activity characterized in earlier research [10,13,18,27,28,35] with semi-purified fractions represents the activity of USP which exhibits broad substrate specifity, a substrate specific UDP-GlcA pyrophosphorylase (EC 2.7.7.44), or a combination of both enzymes. In these earlier studies, the enzyme was not purified and substrate specificity was not thoroughly examined. The most purified fractions exhibiting UDP-GlcA pyrophosphorylase activity were obtained from barley seedlings (80-fold purification) [27] and common cattail pollen (600-fold purification) [18]. The barley UDP-GlcA pyrophosphorylase activity characterized by Roberts [27] cannot be attributed to USP because the enzyme had an estimated molecular wt of 35 kDa and did not cross-react with UDP-Glc. However, the UDP-GlcA pyrophosphorylase characterized from common cattail pollen exhibited properties similar to AtUSP [18]. The common cattail enzyme has a molecular wt of approximately 71 kDa and an apparent $K_m$ value for GlcA-1-P that is in close agreement with values observed for AtUSP.

The expression of USP has not been previously characterized. Our results indicate that USP enzyme activity (UDP-GlcA → GlcA-1-P) and transcript are widely expressed throughout development in Arabidopsis tissues. Both enzyme activity and transcript levels showed high expression in the inflorescence. Although high levels of *USP* transcript and enzyme activity were measured in the inflorescence, we cannot be certain that the enzyme activity measured solely represents the activity of the *USP* gene product. It is possible that the extracts in which enzyme activity was measured contain other pyrophosphorylases capable of catalyzing the conversion of UDP-GlcA to GlcA-1-P.

Histochemical analysis of plants transformed with *AtUSP-prom:GUS* demonstrated high expression in specific tissues, including epidermis, trichomes, cotyledons and vascular tissues. High levels of GUS expression were also detected in pollen. *In silico* analysis indicated that *AtUSP* transcript is highest in the stamen and that transcript increases as pollen development progresses from the uninucleate to tricellular stage. Although these results suggest that USP may be important in pollen development, its exact role is not clear. It is possible that USP is required because of its proposed salvage function in nucleotide sugar synthesis [22]. Alternatively, if USP serves as the terminal enzyme of the MIO pathway, it may play an important role in pollen development by providing UDP-GlcA, a key prescuror for synthesis of cell wall matrix polysaccharides. If this is the case, USP may contribute to the synthesis of the intine, the pectocellulosic inner wall of developing pollen [30]. The intine is formed as pollen development progresses from the uninucleate to the tricellular stage [2].

Previous research has suggested that the MIO pathway and UDP-GlcA PPase may be important in pollen. Relatively high levels of UDP-GlcA pyrophosphorylase activity were measured in mature pollen of common cattail [18] and in germinating pollen of lily [10,28]. Other evidence that the MIO pathway may be active in pollen is the finding that one of the *myo*-inositol oxidase genes (MIOX 4) is highly expressed in Arabidopsis pollen [20]. These authors concluded that the MIO pathway may play a major role in the biosynthesis of UDP-GlcA in Arabidopsis pollen. Further research will be needed to define the role of USP in the salvage pathway for nucleotide sugar synthesis and its possible contribution to *de novo* synthesis of UDP-GlcA via the MIO pathway. The availability of Arabidopsis knock-out lines for *USP* and the fact that Arabidopsis contains a single *USP* gene will allow for research to better define the role of *AtUSP* in pollen and other plant tissues.

## 4. Materials and methods

### 4.1. Chemicals

Radiolabeled substrates, [$^{14}$C]UDP-GlcA ($1.16 \times 10^{10}$ Bq mmol$^{-1}$) and [$^{14}$C]UDP-Glc ($1.12 \times 10^{10}$ Bq mmol$^{-1}$)] were purchased from MP Biomedicals (Irvine, CA). All other chemicals were purchased from Sigma-Aldrich (St. Louis, MO). Mention of trade names or commercial products in this publication is solely for the purpose of providing specific information and does not imply recommendation or endorsement by the U.S. Department of Agriculture.

### 4.2. Plant growth conditions

For experiments conducted with 7-day-old seedlings of *Arabidopsis thaliana* (ecotype Columbia), sterilized seed were grown on solidified medium [MS Salts, 1% (w/v) sucrose, 3.5 g l$^{-1}$ Phytagel, pH 5.7]. For all other experiments, Arabidopis (ecotype Columbia or transgenic plants) was grown on Sunshine Mix LP5 (SunGro Horticulture, Bellevue, WA). Plants were grown under a 24 h photoperiod at 21 ± 2 °C.

### 4.3. Cloning, expression and purification of AtUSP

The coding region corresponding to the At5g52560 locus was cloned using RT-PCR. Gene specific primers were selected from the 5′- and 3′-untranslated regions of expressed sequence contig TC211316 <http://www.tigr.org> (5′-TTGTTAAGAGCCTCTTCA-3′, 5′-AATGTGCAAAGA TAACTT-3′). Total RNA from whole plants was used as the template for cDNA synthesis with the 3′ gene-specific primer and AMV reverse transcriptase (Promega, Madison, WI). Nucleotides and enzymes were removed after each step by washing on spin columns (Qiagen, Valencia, CA). The coding

sequence was amplified from the cDNA using *Pfx* DNA polymerase (Invitrogen, Carlsbad, CA) which yielded a product of approximately 2.5 kb. This product was incubated with dATP and Taq polymerase to add terminal overhangs, then ligated into pGEM-T Easy (Promega).

The coding region of *AtUSP* was cloned into expression vector pET28b (Novagen, San Diego, CA) and transformed into *E. coli* strain BL21pLysS. Cultures were grown in LB medium at 37 °C to an optical density of 0.6, then induced by addition of 1 mM isopropyl-β-thiogalactoside. After induction, the cultures were incubated at 22 °C for 5 h. Cells were harvested by centrifugation (8,000g, 15 min) and resuspended in 1/20 culture volume of lysis buffer [0.4 M NaCl, 100 mM HEPES, 10 mM imidazole, 5 mM DTT (pH 7.5)] with 2 units $ml^{-1}$ DNase (Sigma-Aldrich), and then frozen at –20 °C. Uninduced cultures or control cultures with an empty vector gave no detectable UDP-GlcA pyrophosphorylase activity.

AtUSP was purified from the soluble cytoplasmic protein fraction by binding to His-Link affinity resin (Promega) according to the manufacturer's instructions. AtUSP was eluted with a buffer containing 500 mM imidazole, 10 mM HEPES (pH 7.5) and 1 mM DTT. The fraction was then desalted on a PD-10 column (Amersham Biosciences, Piscataway, NJ) equilibrated with buffer [20% (w/v) sucrose, 50 mM TAPS (pH 8.0), 1 mM $MgCl_2$, 1 mM DTT]. At this point no other proteins could be detected by silver staining a SDS-PAGE gel. After purification, the poly-His tag was removed by thrombin cleavage for 16 h at 4 °C with 1 unit thrombin per mg AtUSP. Thrombin was removed by affinity chromatography according to the manufacturer's instructions (Novagen). Protein concentrations were determined using the method of Bradford [6] with BSA as the standard.

### 4.4. USP assays and kinetic analyses

USP activity was measured in both the forward direction (conversion of GlcA-1-P to UDP-GlcA) and in the reverse direction (conversion of [$^{14}$C]UDP-GlcA to [$^{14}$C]GlcA- 1-P). For the forward reaction involving the conversion of GlcA-1-P to UDP-GlcA, Pi formation was measured after hydrolysis of PPi by pyrophosphatase. The assay medium contained 10 mM TAPS (pH 8.0), 2 mM $MgCl_2$, 1.67 nkat $ml^{-1}$ inorganic pyrophosphatase, 1 mM UTP and 1 mM sugar-phosphate substrate. Inorganic pyrophosphatase activity was in excess of that needed to completely hydrolyze PPi produced in the assay. The reaction was started by addition of recombinant enzyme (100 ng) in a final reaction volume of 0.5 ml. After incubating 10 min at 30 °C, formation of Pi was detected by the method of Aoyama et al. [1]. An equal volume of 3% (w/v) ammonium molybdate and 0.1 volume of 1% (w/v) ascorbic acid, both made up in 200 mM Na acetate buffer (pH 4.0), was added. Color was allowed to develop for 30 min at room temperature and absorbance at 720 nm was measured. A standard curve prepared in assay buffer gave a linear reaction over the range of 0-250 μM Pi.

USP activity in the reverse direction was determined by measuring the formation of [$^{14}$C]GlcA-1-P from UDP-[$^{14}$C]GlcA and inorganic pyrophosphate using a modified protocol of Szumilo et al. [34]. The reaction mixtures contained the following components in a final volume of 50 μl: 100 mM TAPS (pH 8.0), 2 mM $MgCl_2$, 2 mM UDP-[$^{14}$C]GlcA ($1.85 \times 10^7$ Bq $mmol^{-1}$), 5 mM sodium pyrophosphate and purified recombinant enzyme. After a 10 min incubation at 30 °C, the reactions were terminated by adding 0.5 ml 5% (w/v) TCA. Nucleotides were adsorbed on charcoal by adding 0.3 ml ENVI-Carb 120/400 (Sigma-Aldrich, St. Louis, MO) (150 mg $ml^{-1}$ in water). The suspension was shaken for 2 min and the charcoal pelleted by centrifugation (16,000*g*, 2 min). The supernatant was removed and saved, and the charcoal was washed with 1.0 ml water. The supernatants were combined and 1.0 ml was added to 15 ml EcoLume for scintillation counting. Blank controls were run simultaneously and contained all components with the exception of sodium pyrophosphate.

The formation of [$^{14}$C]GlcA-1-P in the reverse assay was verified by separating the reaction products on cellulose TLC plates. The reverse assay was stopped by adding 2 μl 0.5 M EDTA, and 2 μl of the reaction mixture was applied to a Cellulose 300 flexible-backed TLC plate (Selecto Scientific). The plate was developed with n-butanol:acetone:acetic acid:5% ammonium hydroxide:water (3.5:2.5:1.5:1.5:1) [26]. The standard lanes, containing 20 nmol of either UDP-GlcA or GlcA-1-P, were sprayed with an acidic molybdate spray (1% ammonium molybdate, 3% perchloric acid and 0.1N HCl) to detect phosphate esters [4,5]. The corresponding bands from the reaction lanes were cut out and placed in 7 ml scintillation vials with 0.2 ml water. After vortexing, 5 ml of EcoLume was added for scintillation counting.

The non-radioactive forward assay (GlcA-1-P → UDP-GlcA) described above was modified for determination of kinetic parameters. Inorganic pyrophosphatase was omitted from the assay medium. After the 10 min incubation at 30 °C with 100 ng of purified AtUSP, the reaction was stopped by boiling for 2.5 min. The samples were then placed on ice to cool. Inorganic pyrophosphatase [50 μl of 16.7 nkat $ml^{-1}$ in 50% (v/v) glycerol] was added and the samples were incubated for 10 min at 30 °C to cleave PPi. Phosphate was measured as described above. $K_m$ and $V_{max}$ for GlcA-1-P, Glc-1-P and UTP were determined by varying the concentration of UTP from 0.025 to 0.5 mM at each of five fixed concentrations of GlcA-1-P or Glc-1-P (0.1 to 2.0 mM). The data was fitted to an equation describing a two substrate ping pong mechanism using non-linear regression software (GraFit 3.0, Erithacus Software). $K_m$ and $V_{max}$ for UDP-GlcA and UDP-Glc were determined by varying the concentration of UDP-sugar from 0.1 to 2 mM at a fixed concentration of NaPPi (1 mM). $K_m$ and $V_{max}$ for PPi were determined by varying the concentration of PPi from 0.1 to 1 mM at a fixed concentration of either UDP-GlcA or UDP-Glc (2 mM). The data was fitted to the Michaelis-Menten equation using non-linear regression software (GraFit 3.0). The concentrations of fixed substrates were empirically determined to be saturating.

### 4.5. Determination of USP activity in plant extracts

Approximately 1 g fresh wt of tissue was ground with sand using a mortar and pestle in 5 ml extraction buffer [50 mM Tris-Cl (pH 8.0), 1 mM $MgCl_2$, 0.5 M KCl, 0.1% (v/v) Triton X-100, 0.07% (v/v) β-mercaptoethanol, 0.5 mM phenylmethanesulfonyl fluoride] and then filtered through cheesecloth and Miracloth. Extracts were centrifuged at 12,000*g* for 10 min at 4 °C. After filtering through Miracloth, 2.5 ml of supernatant was loaded onto a PD-10 column (Amersham Pharmacia Biotech, Piscataway, NJ) pre-equilibrated in desalting buffer [50 mM Tris-Cl (pH 8.0), 1 mM $MgCl_2$, 10% (v/v) glycerol, 0.07% (v/v) β-mercaptoethanol]. Eluate was collected after 3.5 ml desalting buffer was added to the column. Desalted crude extracts (20 μl) were used in the USP reverse assay (UDP- [$^{14}$C]GlcA → [$^{14}$C] GlcA-1-P). Assay conditions were the same as described above except the reaction time was 30 min and the nucleotide binding step was modified. Reactions were stopped with 0.5 ml 5% (w/v) TCA and 0.3 ml ENVI-Carb 120/400 (150 mg $ml^{-1}$ in water) was added. After 2 min of mixing, the entire mixture was loaded onto a 2 ml, 0.2 μm nylon filter spin unit (Chrom Tech, Inc., AppleValley, MN). After a 1 min spin at 1000*g*, 0.5 ml was counted in 10 ml EcoLume.

### 4.6. RNA expression analysis

Total RNA was extracted from 100 to 150 mg of tissue using Trizol reagent (Invitrogen, Carlsbad, CA) according to manufacturer's protocol and then treated with DNase at 37 °C for 30 min in a 200 μl reaction containing 5 units $ml^{-1}$ RQ1 DNase (Promega), 200 units $ml^{-1}$ RNasin (Promega), 50 mM Tris (pH 7.8), 10 mM $MgCl_2$ and 1 mM DTT. The RNA was extracted from the DNase reaction with phenol:chloroform (1:1, v/v), then ethanol precipitated prior to use in the RT reaction. For each sample, reverse transcription was carried out in a 20 μl reaction using 1 μg of total RNA and ImpromII Reverse Transcriptase (Promega) according to the manufacturer's instructions. The reaction was then diluted with 20 μl of water to give a final volume of 40 μl of cDNA. Multiplex PCR reactions were conducted with 2 μl of the diluted cDNA in a volume of 20 μl. The reactions were carried out according to the QuantumRNA 18S Internal Standards Kit (Ambion, Austin, TX) using the Quantum 18S Universal standards (4:6 ratio of 18Sprimers:18Scompetimers) to amplify a 315 bp fragment of 18S ribosomal DNA, and two primers (5′-GGAAGCTATTG GAGGAATTAG-3′ and 5′-GACACCAGCCTTTTGAAGAA-3′) designed to amplify a 450 bp fragment of *AtUSP*. The resulting PCR reactions were run on a 2% agarose gel, stained with ethidium bromide and the bands were quantified using the BioRad Doc 2000 gel documentation system with Quantity One (version 4.1.1) software from BioRad (Hercules, CA).

*In silico* expression analysis was performed at https://www.genevestigator.ethz.ch/ using Gene Atlas [37]. For the Arabidopsis organ profile, only wild-type (Col-0) data sets on ATH1: 22 k arrays were chosen. Developing pollen arrays were only available from RNA isolated from the Landsberg erecta ecotoype. Data is current as of November, 2005.

### 4.7. Histochemical GUS analysis

To determine tissue-specific expression of *AtUSP*, 2.0 kb immediately upstream of the At5g52560 start codon was amplified with USPpromL (5′-GCTCTAGAGTTATCCTTT GAAAGCATTCGTCC-3′) and USPpromR (5′-GCTCTAGA GAAGAGGCTCTTAACAAAGGAATG-3′) primers using wild-type (Col) genomic DNA with Expand High Fidelity PCR System (Roche Applied Sciences, Germany). The gel-purified PCR product (Qiagen) was digested with *Xba*I and ligated into a promoterless-GUS contruct (pBI101.1) resulting in the transformation vector pJS1. *Agrobacterium* (GV3101) harboring pJS1 were used to transform wild-type (Col) Arabidopsis plants according to Clough and Bent [9]. Two independent transformation events were used in the analysis of promoter activity. Kanamycin-resistant seedlings were selected on Germination Medium (MS salts, 1% (w/v) sucrose, 3.5 g $l^{-1}$ Phytagel, 75 mg $l^{-1}$ kanamycin, pH 5.6) after 10 days. Histochemical GUS assays were performed as described [19]. Assay buffer was vacuum infiltrated into tissues and allowed to incubate at 37 °C overnight. Tissues were cleared in 70% ethanol.

## Acknowledgments

We thank Ann Chaptman and Renee Schirmer for technical assistance.

## References

[1] H. Aoyama, A.D.M. Cavagis, E.M. Taga, C.V. Ferreira, Endogenous lectin as a possible regulator of the hydrolysis of physiological substrates by soybean seed acid phosphatase, Phytochemistry 58 (2001) 221–225.

[2] T. Ariizumi, K. Hatakeyama, K. Hinata, R. Inatsugi, I. Nishida, S. Sato, T. Kato, S. Tabata, K. Toriyama, Disruption of the novel protein NEF1 affects lipid accumulation in the plastids of the tapetum and exine formation of pollen, resulting in male sterility in *Arabidopsis thaliana*, Plant J. 39 (2004) 170–181.

[3] A. Bacic, P.J. Harris, B.A. Stone, Structure and function of plant cell walls, in: P.K. Stumpf, E.E. Conn (Eds.), The Biochemistry of Plants: A Comprehensive Treatise, Vol. 14, Academic Press, 1988, pp. 297–371.

[4] R.S. Bandurski, B. Axelrod, The chromatographic identification of some biologically important phosphate esters, J. Biol. Chem. 193 (1951) 405–410.

[5] R.L. Bieleski, R.E. Young, Extraction and separation of phosphate esters from plant tissues, Anal. Biochem. 6 (1963) 54–68.

[6] M.M. Bradford, A rapid and sensitive method for the quantitation of microgram quantities of protein utilizing the principle of protein-dye binding, Anal. Biochem. 72 (1976) 248–254.

[7] N.C. Carpita, R.A. Brown, K.M. Weller, Uptake and metabolic fate of glucose, arabinose, and xylose by *Zea mays* coleoptiles in relation to cell wall synthesis, Plant Physiol. 69 (1982) 1173–1180.

[8] N. Carpita, M. McCann, The Cell Wall, in: B.B. Buchanan, W. Gruissem, R.L. Jones (Eds.), Biochemistry and Molecular Biology of Plants, American Society of Plant Physiologists, 2000, pp. 52–108.

[9] S.J. Clough, A.F. Bent, Floral dip: a simplified method for Agrobacterium-mediated transformation of *Arabidopsis thaliana*, Plant J. 16 (1998) 735–743.

[10] D.B. Dickinson, D. Hyman, J.W. Gonzales, Isolation of uridine 5'-pyrophosphate glucuronic acid pyrophosphorylase and its assay using $^{32}$P-pyrophosphate, Plant Physiol. 59 (1977) 1082–1084.
[11] O. Emanuelsson, H. Nielsen, S. Brunak, G. von Heijne, Predicting subcellular localization of proteins based on their N-terminal amino acid sequence, J. Mol. Biol. 300 (2000) 1005–1016.
[12] D.S. Feingold, G. Avigad, Sugar nucleotide transformations in plants, in: P.K. Stumpf, E.E. Conn (Eds.), The Biochemistry of Plants: A Comprehensive Treatise, Vol. 3, Academic Press, 1980, pp. 101–170.
[13] D.S. Feingold, E.F. Neufeld, W.Z. Hassid, Enzymic synthesis of uridine diphosphate glucuronic acid and uridine diphosphate galacturonic acid with extracts from *Phaseolus aureus* seedlings, Arch. Biochem. Biophys. 78 (1958) 401–406.
[14] D.M. Gibeaut, Nucleotide sugars and glycosyltransferases for synthesis of cell wall matrix polysaccharides, Plant Physiol. Biochem. 38 (2000) 69–80.
[15] D.M. Gibeaut, N.C. Carpita, Tracing cell wall biogenesis in intact cells and plants: Selective turnover and alteration of soluble and cell wall polysaccharides in grasses, Plant Physiol. 97 (1991) 551–561.
[16] T.A. Gorshkova, S.B. Chemikosova, V.V. Lozovaya, N.C. Carpita, Turnover of galactans and other cell wall polysaccharides during development of flax plants, Plant Physiol. 114 (1997) 723–729.
[17] B. Hinterberg, C. Klos, R. Tenhaken, Recombinant UDP-glucose dehydrogenase from soybean, Plant Physiol. Biochem. 40 (2002) 1011–1017.
[18] T. Hondo, A. Hara, T. Funaguma, Purification and properties of UDP-glucuronate pyrophosphorylase from pollen of *Typha latifolia* Linne, Plant Cell Physiol. 24 (1983) 1535–1543.
[19] R.A. Jefferson, Assaying chimeric genes in plants: The GUS gene fusion system, Plant Mol. Biol. Rep. 5 (1987) 387–405.
[20] U. Kanter, B. Usadel, F. Guerineau, Y. Li, M. Pauly, R. Tenhaken, The inositol oxygenase gene family of *Arabidopsis* is involved in the biosynthesis of nucleotide sugar precursors for cell-wall matix polysaccharides, Planta 221 (2005) 243–254.
[21] A. Kärkönen, Biosynthesis of UDP-GlcA: Via UDPGDH or the *myo*-inositol oxidation pathway?, Plant Biosyst. 139 (2005) 46–49.
[22] T. Kotake, D. Yamaguchi, H. Ohzono, S. Hojo, S. Kaneko, H. Ishida, Y. Tsumuraya, UDP-sugar pyrophosphorylase with broad substrate specificity toward various monosaccharide 1-phosphates from pea sprouts, J. Biol. Chem. 279 (2004) 45728–45736.
[23] F.A. Loewus, M.W. Loewus, *myo*-Inositol: Its biosynthesis and metabolism, Ann. Rev. Plant Physiol. 34 (1983) 137–161.
[24] K. Otozai, H. Taniguchi, M. Nakamura, UDP-glucose pyrophosphorylase from tubers of Jerusalem artichoke (*Helianthus tuberosus* L.), Agr. Biol. Chem. 37 (1973) 531–537.
[25] C. Petit, G.P. Rigg, C. Pazzani, A. Smith, V. Sieberth, M. Stevens, G. Boulnois, K. Jann, I.S. Roberts, Region 2 of the *Escherichia coli* K5 capsule gene cluster encoding proteins for the biosynthesis of the K5 polysaccharide, Mol. Microbiol. 17 (1995) 611–620.
[26] K. Randerath, A comparison between thin-layer chromatography and paper chromatography of nucleic acid derivatives, Biochem. Biophys. Res. Commun. 6 (1962) 452–457.
[27] R.M. Roberts, The formation of uridine diphosphate-glucuronic acid in plants: Uridine diphosphate-glucuronic acid pyrophosphorylase from barley seedlings, J. Biol. Chem. 246 (1971) 4995–5002.
[28] R.M. Roberts, J.J. Cetorelli, UDP-D-Glucuronic acid pyrophosphorylase and the formation of UDP-D-glucuronic acid in plants, in: F. Loewus (Ed.), Biogenesis of Plant Cell Wall Polysaccharides, Academic Press, New York, 1973, pp. 49–68.
[29] D.A. Samac, L. Litterer, G. Temple, H.-J.G. Jung, D.A. Somers, Expression of UDP-glucose dehydrogenase reduces cell-wall polysaccharide concentration and increases xylose content in alfalfa stems, Appl. Biochem. Biotechnol. 116 (2004) 1167–1182.
[30] R.J. Scott, M. Spielman, H.G. Dickinson, Stamen structure and function, Plant Cell 16 (2004) S46–S60.
[31] J.R. Sowokinos, J.P. Spychalla, S.L. Desborough, Pyrophosphorylases in *Solanum tuberosum*. IV. Purification, tissue localization, and physiochemical properties of UDP-glucose pyrophosphorylase, Plant Physiol. 101 (1993) 1073–1080.
[32] A.P. Spicer, L.A. Kaback, T.J. Smith, M.F. Seldin, Molecular cloning and characterization of the human and mouse UDP-glucose dehydrogenase genes, J. Biol. Chem. 273 (1998) 25117–25124.
[33] D.C. Stewart, L. Copeland, Uridine 5'-diphosphate-glucose dehydrogenase from soybean nodules, Plant Physiol. 116 (1998) 349–355.
[34] T. Szumilo, Y. Zeng, I. Pastuszak, R. Drake, H. Szumilo, A.D. Elbein, Purification to homogeneity and properties of UDP-GlcNAc (GalNAc) pyrophosphorylase, J. Biol. Chem. 271 (1996) 13147–13154.
[35] H.-J. Witt, UDP-glucose metabolism during differentiation and dedifferentiation of *Riella helicophylla*, J. Plant Physiol. 140 (1992) 276–281.
[36] E. Zablackis, J. Huang, B. Müller, A.G. Darvill, P. Albersheim, Characterization of the cell-wall polysaccharides of *Arabidopsis thaliana* leaves, Plant Physiol. 107 (1995) 1129–1138.
[37] P. Zimmermann, M. Hirsch-Hoffmann, L. Hennig, W. Gruissem, GENEVESTIGATOR. Arabidopsis microarray database and analysis toolbox, Plant Physiol. 136 (2004) 2621–2632.